Novel analytical solutions for bending, buckling and vibration analysis of laminated composite beams

Ngoc-Duong Nguyen[a], Trung-Kien Nguyen[a,*], Thuc P. Vo[b,c], Huu-Tai Thai[d]

[a] Faculty of Civil Engineering, Ho Chi Minh City University of Technology and Education, 1 Vo Van Ngan Street, Thu Duc District, Ho Chi Minh City, Viet Nam

[b] Institute of Research and Development, Duy Tan University, 03 Quang Trung, Da Nang, Viet Nam

[c] Faculty of Engineering and Environment, Northumbria University, Newcastle upon Tyne, NE1 8ST, UK

[d] School of Engineering and Mathematical Sciences, La Trobe University, Bundoora, VIC 3086, Australia

Abstract

In this paper, Ritz-based solutions are developed for bending, buckling and vibration analysis of laminated composite beams with arbitrary lay-ups. A quasi-3D theory which accounts for a higher-order variation of both axial and transverse displacements is used to capture the effects of both shear and normal deformations on the behaviors of composite beams. Numerical results for various boundary conditions are presented to compare with existing solutions, and to investigate the effects of fiber angle, span-to-height ratio, material anisotropy and Poisson's ratio on the displacements, stresses, natural frequencies and buckling loads of composite beams.

Keywords: Analytical approach; Static; Vibration; Buckling; Laminated composite beams.

1. Introduction

Composite materials are used commonly in many engineering fields due to their high strength-to-weight and stiffness-to-weight ratios as well as the ability to customize fiber

[*] Corresponding author. Tel.: + 848 3897 2092.
E-mail address: kiennt@hcmute.edu.vn (T-K Nguyen)

orientations to meet design requirements. A large number of beam models have been developed to predict the structural behavior of composite beams [1]. It is noted that the classical beam theory (CBT) [2, 3] is only suitable for the analysis of slender beams due to neglecting the shear effect. The first-order beam theory (FOBT) [4-9] overcomes this drawback by assuming shear stress distribution to be constant through the height. Thus, a shear correction factor is required to correct this inadequate variation. To avoid the inconsistency of the FOBT, higher-order beam theories (HOBTs) with higher-order variations of axial displacement are developed [10-14]. The HOBT predicts the behaviors of composite beams more accurate than the FOBT. However, the effect of transverse normal strain is neglected. For this reason, quasi-3D theories [15-18] were developed based on higher-order variations of both axial and transverse displacements.

For computational methods, many analytical and numerical approaches have been proposed to analyze behaviors of composite beams and only some of them using HOBTs are mentioned here. Zenkour [15] used Navier solutions for the bending analysis of cross-ply laminated and sandwich beams. Aydogdu [19-21] developed Ritz solutions for the buckling and vibration analysis of composite beams. Mantari and Canales [22, 23] also analyzed the vibration and buckling responses of composite beams by using the Ritz method. Nguyen et al. [24] proposed a Ritz solution for composite beams by using trigonometric functions. Khdeir and Reddy [25, 26] adopted the state-space approach for the vibration and buckling analysis of cross-ply laminated beams. The analytical solution was derived by Teh and Huang [27] to investigate the effects of fiber orientation on the free vibration of composite beams. Finite element method has also been widely used to analyze static, dynamic and buckling of composite beams [28-38]. In addition, dynamic stiffness matrix method was used by Jun et al. [39] for the vibration analysis of composite beams. Shao et al. [40] used the reverberation-ray matrix method to analyze the free vibration of composite beams with general boundary conditions. Although Ritz method is efficient to analyze the behaviors of composite beams with various boundary conditions, the available literature indicated that the number of works used the Ritz method is still limited [19-24]. Among them, only a few research investigated the effects of both transverse and normal strains on the static, vibration and buckling behaviors of composite beams. Unlike the cross-ply lay-ups, composite beams with arbitrary ones, which considered in this study, have the coupling effect between out-of-plane stresses and strains and thus it is more complicated and needs further studies.

The objective of this study is to propose novel Ritz solutions for the static, vibration and buckling analysis of composite beams with arbitrary lay-ups based on a quasi-3D theory. The governing equations of motion are derived by using Lagrange's equations. The convergence and verification studies are carried out to demonstrate the accuracy of the present study. Numerical results are presented to investigate the effects of transverse and normal strains, span-to-height ratio, fiber angle, Poisson's ratio and material anisotropy on the deflections, stresses, natural frequencies and buckling loads of composite beams.

2. Theoretical formulation

A rectangular composite beam with cross-section ($b \times h$) and length L as shown in Fig. 1 is considered. It is made of n plies of orthotropic materials in different fibre angles with respect to the x-axis.

2.1. Kinetic, strain and stress relations

The displacement field of a quasi-3D theory proposed by Zenkour [15] is adopted herein:

$$u(x,z,t) = u_0(x,t) + zu_1(x,t) - \frac{1}{2}z^2\frac{\partial w_1}{\partial x} + z^3\left[-\frac{4}{3h^2}\left(\frac{\partial w_0}{\partial x} + u_1(x,t)\right) - \frac{1}{3}\frac{\partial w_2}{\partial x}\right] \tag{1a}$$

$$w(x,z,t) = w_0(x,t) + zw_1(x,t) + z^2 w_2(x,t) \tag{1b}$$

where $u_0(x,t)$ and $w_0(x,t)$ are the axial and transverse displacements of mid-plane of the beam, respectively; $u_1(x,t)$ is the rotation about the y-axis; $w_1(x,t)$ and $w_2(x,t)$ are additional higher-order terms. The present theory has 5 unknown variables, which need to be determined.

The strain field of beams is given by:

$$\varepsilon_x = \frac{\partial u}{\partial x} = \varepsilon_x^{(0)} + z\varepsilon_x^{(1)} + z^2\varepsilon_x^{(2)} + z^3\varepsilon_x^{(3)} \tag{2a}$$

$$\varepsilon_z = \frac{\partial w}{\partial z} = \varepsilon_z^{(0)} + z\varepsilon_z^{(1)} \tag{2b}$$

$$\gamma_{xz} = \frac{\partial u}{\partial z} + \frac{\partial w}{\partial x} = \gamma_{xz}^{(0)} + z^2\gamma_{xz}^{(1)} \tag{2c}$$

where

$$\varepsilon_x^{(0)} = \frac{\partial u_0}{\partial x},\quad \varepsilon_x^{(1)} = \frac{\partial u_1}{\partial x},\quad \varepsilon_x^{(2)} = -\frac{1}{2}\frac{\partial^2 w_1}{\partial x^2},\quad \varepsilon_x^{(3)} = \left[-\frac{4}{3h^2}\left(\frac{\partial^2 w_0}{\partial x^2} + \frac{\partial u_1}{\partial x}\right) - \frac{1}{3}\frac{\partial^2 w_2}{\partial x^2}\right] \tag{3a}$$

$$\varepsilon_z^{(0)} = w_1,\quad \varepsilon_z^{(1)} = 2w_2,\quad \gamma_{xz}^{(0)} = u_1 + \frac{\partial w_0}{\partial x},\quad \gamma_{xz}^{(2)} = -\frac{4}{h^2}\left(u_1 + \frac{\partial w_0}{\partial x}\right) \tag{3b}$$

The elastic strain and stress relation of the k^{th}-layer in a global coordinate is given by:

$$\begin{Bmatrix} \sigma_x \\ \sigma_y \\ \sigma_z \\ \sigma_{yz} \\ \sigma_{xz} \\ \sigma_{xy} \end{Bmatrix}^{(k)} = \begin{pmatrix} \overline{C}_{11} & \overline{C}_{12} & \overline{C}_{13} & 0 & 0 & \overline{C}_{16} \\ \overline{C}_{12} & \overline{C}_{22} & \overline{C}_{23} & 0 & 0 & \overline{C}_{26} \\ \overline{C}_{13} & \overline{C}_{23} & \overline{C}_{33} & 0 & 0 & \overline{C}_{36} \\ 0 & 0 & 0 & \overline{C}_{44} & \overline{C}_{45} & 0 \\ 0 & 0 & 0 & \overline{C}_{45} & \overline{C}_{55} & 0 \\ \overline{C}_{16} & \overline{C}_{26} & \overline{C}_{36} & 0 & 0 & \overline{C}_{66} \end{pmatrix}^{(k)} \begin{Bmatrix} \varepsilon_x \\ \varepsilon_y \\ \varepsilon_z \\ \gamma_{yz} \\ \gamma_{xz} \\ \gamma_{xy} \end{Bmatrix} \tag{4}$$

where the $\overline{C}_{ij}$ are transformed elastic coefficients [41]. Moreover, a plane stress constitutive relation in the y-direction can be assumed for composite beams. By setting $\sigma_y = \sigma_{xy} = \sigma_{yz} = 0$, Eq. (4) is reduced to:

$$\begin{Bmatrix} \sigma_x \\ \sigma_z \\ \sigma_{xz} \end{Bmatrix}^{(k)} = \begin{pmatrix} \overline{\overline{C}}_{11} & \overline{\overline{C}}_{13} & 0 \\ \overline{\overline{C}}_{13} & \overline{\overline{C}}_{33} & 0 \\ 0 & 0 & \overline{\overline{C}}_{55} \end{pmatrix}^{(k)} \begin{Bmatrix} \varepsilon_x \\ \varepsilon_z \\ \gamma_{xz} \end{Bmatrix} \tag{5}$$

where $\overline{\overline{C}}_{11}, \overline{\overline{C}}_{13}, \overline{\overline{C}}_{33}, \overline{\overline{C}}_{55}$ are reduced stiffness constants of k^{th}-layer in global coordinates, which are related to $\overline{C}_{ij}$ as follows:

$$\overline{\overline{C}}_{11} = \overline{C}_{11} + \frac{\overline{C}_{16}^2 \overline{C}_{22} - 2\overline{C}_{12}\overline{C}_{16}\overline{C}_{26} + \overline{C}_{12}^2 \overline{C}_{66}}{\overline{C}_{26}^2 - \overline{C}_{22}\overline{C}_{66}} \tag{6a}$$

$$\overline{\overline{C}}_{13} = \overline{C}_{13} + \frac{\overline{C}_{16}\overline{C}_{22}\overline{C}_{36} + \overline{C}_{12}\overline{C}_{23}\overline{C}_{66} - \overline{C}_{16}\overline{C}_{23}\overline{C}_{26} - \overline{C}_{12}\overline{C}_{26}\overline{C}_{36}}{\overline{C}_{26}^2 - \overline{C}_{22}\overline{C}_{66}} \tag{6b}$$

$$\overline{\overline{C}}_{33} = \overline{C}_{33} + \frac{\overline{C}_{36}^2 \overline{C}_{22} - 2\overline{C}_{23}\overline{C}_{26}\overline{C}_{36} + \overline{C}_{23}^2 \overline{C}_{66}}{\overline{C}_{26}^2 - \overline{C}_{22}\overline{C}_{66}} \tag{6c}$$

$$\overline{\overline{C}}_{55} = \overline{C}_{55} - \frac{\overline{C}_{45}^2}{\overline{C}_{44}} \tag{6d}$$

If the transverse normal stress is omitted ($\sigma_z = 0$), the strain and stress relations of a HOBT are recovered as:

$$\begin{Bmatrix} \sigma_x \\ \sigma_{xz} \end{Bmatrix}^{(k)} = \begin{pmatrix} \bar{\bar{C}}^{*}_{11} & 0 \\ 0 & \bar{\bar{C}}^{*}_{55} \end{pmatrix}^{(k)} \begin{Bmatrix} \varepsilon_x \\ \gamma_{xz} \end{Bmatrix} \tag{7}$$

where $\bar{\bar{C}}^{*}_{11} = \bar{\bar{C}}_{11} - \frac{\bar{\bar{C}}^{2}_{13}}{\bar{\bar{C}}_{33}}$, $\bar{\bar{C}}^{*}_{55} = \bar{\bar{C}}_{55}$. It should be noted that for HOBT, the higher-order terms ($w_1(x,t)$ and $w_2(x,t)$) will be vanished.

2.2. Variational formulation

The strain energy U of system is given by:

$$\begin{aligned}
U &= \frac{1}{2}\int_V \left(\sigma_x \varepsilon_x + \sigma_z \varepsilon_z + \sigma_{xz}\gamma_{xz} \right) dV \\
&= \frac{1}{2}\int_0^L \Bigg[A_{11}(u_{0,x})^2 + \left(2B_{11} - \frac{8}{3h^2}E_{11} \right) u_{0,x}u_{1,x} - \frac{8}{3h^2}E_{11}u_{0,x}w_{0,xx} - D_{11}u_{0,x}w_{1,xx} + 2A_{13}u_{0,x}w_1 + 4B_{13}u_{0,x}w_2 \\
&- \frac{2}{3}E_{11}u_{0,x}w_{2,xx} + \left(D_{11} + \frac{16}{9h^4}H_{11} - \frac{8}{3h^2}F_{11} \right)(u_{1,x})^2 + \left(A_{55} - \frac{8}{h^2}B_{55} + \frac{16}{h^4}D_{55} \right)u_1^2 \\
&+ \left(\frac{32}{9h^4}H_{11} - \frac{8}{3h^2}F_{11} \right)u_{1,x}w_{0,xx} + 2\left(A_{55} - \frac{8}{h^2}B_{55} + \frac{16}{h^4}D_{55} \right)u_1 w_{0,x} + \left(\frac{4}{3h^2}G_{11} - E_{11} \right)u_{1,x}w_{1,xx} \\
&+ \left(2B_{13} - \frac{8}{3h^2}E_{13} \right)u_{1,x}w_1 + \left(\frac{8}{9h^2}H_{11} - \frac{2}{3}F_{11} \right)u_{1,x}w_{2,xx} + \left(4D_{13} - \frac{16}{3h^2}F_{13} \right)u_{1,x}w_2 + \frac{16}{9h^4}H_{11}(w_{0,xx})^2 \\
&+ \left(A_{55} - \frac{8}{h^2}B_{55} + \frac{16}{h^4}D_{55} \right)(w_{0,x})^2 + \frac{4}{3h^2}G_{11}w_{0,xx}w_{1,xx} - \frac{8}{3h^2}E_{13}w_{0,xx}w_1 + \frac{8}{9h^2}H_{11}w_{0,xx}w_{2,xx} \\
&- \frac{16}{3h^2}F_{13}w_{0,xx}w_2 + \frac{1}{4}F_{11}(w_{1,xx})^2 - D_{13}w_{1,xx}w_1 + A_{33}w_1^2 + \frac{1}{3}G_{11}w_{1,xx}w_{2,xx} - 2E_{13}w_{1,xx}w_2 \\
&- \frac{2}{3}E_{13}w_{2,xx}w_1 + 4B_{33}w_1w_2 + \frac{1}{9}H_{11}(w_{2,xx})^2 - \frac{4}{3}F_{13}w_{2,xx}w_2 + 4D_{33}w_2^2 \Bigg] dx
\end{aligned} \tag{8}$$

where the stiffness coefficients of the beam are determined as follows:

$$\left(A_{11}, B_{11}, D_{11}, E_{11}, F_{11}, G_{11}, H_{11} \right) = \sum_{k=1}^{n} \int_{z_k}^{z_{k+1}} \bar{\bar{C}}_{11}\left(1, z, z^2, z^3, z^4, z^5, z^6\right) b dz \tag{9a}$$

$$\left(A_{13}, B_{13}, D_{13}, E_{13}, F_{13} \right) = \sum_{k=1}^{n} \int_{z_k}^{z_{k+1}} \bar{\bar{C}}_{13}\left(1, z, z^2, z^3, z^4\right) b dz \tag{9b}$$

$$\left(A_{33}, B_{33}, D_{33} \right) = \sum_{k=1}^{n} \int_{z_k}^{z_{k+1}} \bar{\bar{C}}_{33}\left(1, z, z^2\right) b dz \tag{9c}$$

$$\left(A_{55}, B_{55}, D_{55}\right) = \sum_{k=1}^{n} \int_{z_k}^{z_{k+1}} \overline{\overline{C}}_{55}\left(1, z^2, z^4\right) b dz \tag{9d}$$

The work done V by in-plane compressive load N_0 and transverse load q applied on the bottom surface of the beam is given by:

$$V = \frac{1}{2}\int_0^L N_0 \left(w_{0,x}^2 + \frac{h^2}{6} w_{0,x} w_{2,x} + \frac{h^2}{12} w_{1,x}^2 + \frac{h^4}{80} w_{2,x}^2 \right) dx - \int_0^L q \left(w_0 - \frac{h}{2} w_1 + \frac{h^2}{4} w_2 \right) b dx \tag{10}$$

The kinetic energy K of system is written by:

$$K = \frac{1}{2}\int_V \rho(z)\left(\dot{u}^2 + \dot{w}^2\right) dV$$

$$= \frac{1}{2}\int_0^L \Bigg[I_1 \dot{u}_0^2 - I_3 \dot{u}_0 \dot{w}_{1'x} + \left(I_3 + \frac{16}{9h^4} I_7 - \frac{8}{3h^2} I_5 \right) \dot{u}_1^2 + \left(\frac{32}{9h^4} I_7 - \frac{8}{3h^2} I_5 \right) \dot{u}_1 \dot{w}_{0,x} + \left(\frac{8}{9h^2} I_7 - \frac{2}{3} I_5 \right) \dot{u}_1 \dot{w}_{2,x}$$

$$+ \frac{16}{9h^4} I_7 \dot{w}_{0,x}^2 + I_1 \dot{w}_0^2 + \frac{8}{9h^2} I_7 \dot{w}_{0,x} \dot{w}_{2,x} + 2 I_3 \dot{w}_0 \dot{w}_2 + \frac{1}{4} I_5 \dot{w}_{1,x}^2 + I_3 \dot{w}_1^2 + \frac{1}{9} I_7 \dot{w}_{2,x}^2 + I_5 \dot{w}_2^2) \Bigg] dx \tag{11}$$

where dot-superscript denotes the differentiation with respect to the time t; ρ is the mass density of each layer, and I_1, I_3, I_5, I_7 are the inertia coefficients defined by:

$$\left(I_1, I_3, I_5, I_7\right) = \sum_{k=1}^{n} \int_{z_k}^{z_{k+1}} \rho\left(1, z^2, z^4, z^6\right) b dz \tag{12}$$

The total potential energy of system is expressed by:

$$\Pi = U + V - K \tag{13}$$

Based on the Ritz method, the displacement field is approximated in the following forms:

$$u_0(x,t) = \sum_{j=1}^{m} \varphi_{j,x}(x) u_{0j} e^{i\omega t} \tag{14a}$$

$$u_1(x,t) = \sum_{j=1}^{m} \varphi_{j,x}(x) u_{1j} e^{i\omega t} \tag{14b}$$

$$w_0(x,t) = \sum_{j=1}^{m} \varphi_j(x) w_{0j} e^{i\omega t} \tag{14c}$$

$$w_1(x,t)=\sum_{j=1}^{m}\varphi_j(x)w_{1j}e^{i\omega t} \tag{14d}$$

$$w_2(x,t)=\sum_{j=1}^{m}\varphi_j(x)w_{2j}e^{i\omega t} \tag{14e}$$

where ω is the frequency; $i^2=-1$ the imaginary unit; u_{0j}, u_{1j}, w_{0j}, w_{1j}, w_{2j} are unknown values to be determined; $\varphi_j(x)$ are shape functions. It is noted that the accuracy and efficiency of the Ritz method strictly depend on the choice of these shape functions. An inappropriate choice of shape functions may cause slow convergence rates and numerical instabilities [21]. The shape functions used in the Ritz method should satisfy the specified essential boundary conditions [41]. When the shape functions do not satisfy this requirement, a penalty method can be used to impose the boundary conditions [22]. However, this approach is too computational costs. In this paper, the new shape functions composed of polynomial and exponential forms are proposed. These shape functions are given in Table 1 for simply-supported (S-S), clamped-clamped (C-C) and clamped-free (C-F) beams, and satisfy the boundary conditions (BCs) given in Table 2.

The governing equations of motion can be obtained by substituting Eqs. (14) into Eq. (13) and using Lagrange's equations:

$$\frac{\partial \Pi}{\partial q_j}-\frac{d}{dt}\frac{\partial \Pi}{\partial \dot{q}_j}=0 \tag{15}$$

with q_j representing the values of ($u_{0j}, u_{1j}, w_{0j}, w_{1j}, w_{2j}$), that leads to:

$$\left(\begin{bmatrix} \mathbf{K}^{11} & \mathbf{K}^{12} & \mathbf{K}^{13} & \mathbf{K}^{14} & \mathbf{K}^{15} \\ {}^T\mathbf{K}^{12} & \mathbf{K}^{22} & \mathbf{K}^{23} & \mathbf{K}^{24} & \mathbf{K}^{25} \\ {}^T\mathbf{K}^{13} & {}^T\mathbf{K}^{23} & \mathbf{K}^{33} & \mathbf{K}^{34} & \mathbf{K}^{35} \\ {}^T\mathbf{K}^{14} & {}^T\mathbf{K}^{24} & {}^T\mathbf{K}^{34} & \mathbf{K}^{44} & \mathbf{K}^{45} \\ {}^T\mathbf{K}^{15} & {}^T\mathbf{K}^{25} & {}^T\mathbf{K}^{35} & {}^T\mathbf{K}^{45} & \mathbf{K}^{55} \end{bmatrix} - \omega^2 \begin{bmatrix} \mathbf{M}^{11} & \mathbf{0} & \mathbf{0} & \mathbf{M}^{14} & \mathbf{0} \\ \mathbf{0} & \mathbf{M}^{22} & \mathbf{M}^{23} & \mathbf{0} & \mathbf{M}^{25} \\ \mathbf{0} & {}^T\mathbf{M}^{23} & \mathbf{M}^{33} & \mathbf{0} & \mathbf{M}^{35} \\ {}^T\mathbf{M}^{14} & \mathbf{0} & \mathbf{0} & \mathbf{M}^{44} & \mathbf{0} \\ \mathbf{0} & {}^T\mathbf{M}^{25} & {}^T\mathbf{M}^{35} & \mathbf{0} & \mathbf{M}^{55} \end{bmatrix}\right) \begin{Bmatrix} \mathbf{u_0} \\ \mathbf{u_1} \\ \mathbf{w_0} \\ \mathbf{w_1} \\ \mathbf{w_2} \end{Bmatrix} = \begin{Bmatrix} \mathbf{0} \\ \mathbf{0} \\ \mathbf{F_0} \\ \mathbf{F_1} \\ \mathbf{F_2} \end{Bmatrix} \tag{16}$$

where the components of the stiffness matrix **K** and the mass matrix **M** are given by:

$$K_{ij}^{11} = A_{11}\int_0^L \varphi_{i,xx}\varphi_{j,xx}dx\,,\quad K_{ij}^{12} = \left(B_{11} - \frac{4}{3h^2}E_{11}\right)\int_0^L \varphi_{i,xx}\varphi_{j,xx}dx\,,\quad K_{ij}^{13} = -\frac{4}{3h^2}E_{11}\int_0^L \varphi_{i,xx}\varphi_{j,xx}dx$$

$$K_{ij}^{14} = -\frac{1}{2}D_{11}\int_0^L \varphi_{i,xx}\varphi_{j,xx}dx + A_{13}\int_0^L \varphi_{i,xx}\varphi_j dx\,,\quad K_{ij}^{15} = -\frac{1}{3}E_{11}\int_0^L \varphi_{i,xx}\varphi_{j,xx}dx + 2B_{13}\int_0^L \varphi_{i,xx}\varphi_j dx$$

$$K_{ij}^{22} = \left(D_{11} - \frac{8}{3h^2}F_{11} + \frac{16}{9h^4}H_{11}\right)\int_0^L \varphi_{i,xx}\varphi_{j,xx}dx + \left(A_{55} - \frac{8}{h^2}B_{55} + \frac{16}{h^4}D_{55}\right)\int_0^L \varphi_{i,x}\varphi_{j,x}dx$$

$$K_{ij}^{23} = \left(-\frac{4}{3h^2}F_{11} + \frac{16}{9h^4}H_{11}\right)\int_0^L \varphi_{i,xx}\varphi_{j,xx}dx + \left(A_{55} - \frac{8}{h^2}B_{55} + \frac{16}{h^4}D_{55}\right)\int_0^L \varphi_{i,x}\varphi_{j,x}dx$$

$$K_{ij}^{24} = \left(-\frac{1}{2}E_{11} + \frac{2}{3h^2}G_{11}\right)\int_0^L \varphi_{i,xx}\varphi_{j,xx}dx + \left(B_{13} - \frac{4}{3h^2}E_{13}\right)\int_0^L \varphi_{i,xx}\varphi_j dx$$

$$K_{ij}^{25} = \left(-\frac{1}{3}F_{11} + \frac{4}{9h^2}H_{11}\right)\int_0^L \varphi_{i,xx}\varphi_{j,xx}dx + \left(2D_{13} - \frac{8}{3h^2}F_{13}\right)\int_0^L \varphi_{i,xx}\varphi_j dx$$

$$K_{ij}^{33} = \frac{16}{9h^4}H_{11}\int_0^L \varphi_{i,xx}\varphi_{j,xx}dx + \left(A_{55} - \frac{8}{h^2}B_{55} + \frac{16}{h^4}D_{55}\right)\int_0^L \varphi_{i,x}\varphi_{j,x}dx + N_0\int_0^L \varphi_{i,x}\varphi_{j,x}dx$$

$$K_{ij}^{34} = \frac{2}{3h^2}H_{11}\int_0^L \varphi_{i,xx}\varphi_{j,xx}dx - \frac{4}{3h^2}E_{13}\int_0^L \varphi_{i,xx}\varphi_j dx$$

$$K_{ij}^{35} = \frac{4}{9h^2}H_{11}\int_0^L \varphi_{i,xx}\varphi_{j,xx}dx - \frac{8}{3h^2}F_{13}\int_0^L \varphi_{i,xx}\varphi_j dx + \frac{h^2}{12}N_0\int_0^L \varphi_{i,x}\varphi_{j,x}dx$$

$$K_{ij}^{44} = \frac{1}{4}F_{11}\int_0^L \varphi_{i,xx}\varphi_{j,xx}dx - D_{13}\int_0^L \varphi_{i,xx}\varphi_j dx + A_{33}\int_0^L \varphi_i\varphi_j dx + \frac{h^2}{12}N_0\int_0^L \varphi_{i,x}\varphi_{j,x}dx$$

$$K_{ij}^{45} = \frac{1}{6}G_{11}\int_0^L \varphi_{i,xx}\varphi_{j,xx}dx - E_{13}\int_0^L \varphi_{i,xx}\varphi_j dx - \frac{1}{3}E_{13}\int_0^L \varphi_i\varphi_{j,xx}dx + 2B_{33}\int_0^L \varphi_i\varphi_j dx$$

$$K_{ij}^{55} = \frac{1}{9}H_{11}\int_0^L \varphi_{i,xx}\varphi_{j,xx}dx - \frac{4}{3}F_{13}\int_0^L \varphi_{i,xx}\varphi_j dx + 4D_{33}\int_0^L \varphi_i\varphi_j dx + \frac{h^4}{80}N_0\int_0^L \varphi_{i,x}\varphi_{j,x}dx$$

$$M_{ij}^{11} = I_1\int_0^L \varphi_{i,x}\varphi_{j,x}dx\,,\quad M_{ij}^{14} = -\frac{1}{2}I_3\int_0^L \varphi_{i,x}\varphi_{j,x}dx\,,\quad M_{ij}^{22} = \left(I_3 - \frac{8}{3h^2}I_5 + \frac{16}{9h^4}I_7\right)\int_0^L \varphi_{i,x}\varphi_{j,x}dx$$

$$M_{ij}^{23}=\left(-\frac{4}{3h^2}I_5+\frac{16}{9h^4}I_7\right)\int_0^L\varphi_{i,x}\varphi_{j,x}dx\,,\quad M_{ij}^{25}=\left(-\frac{1}{3}I_5+\frac{4}{9h^2}I_7\right)\int_0^L\varphi_{i,x}\varphi_{j,x}dx$$

$$M_{ij}^{33}=I_1\int_0^L\varphi_i\varphi_j dx+\frac{16}{9h^4}I_7\int_0^L\varphi_{i,x}\varphi_{j,x}dx\,,\quad M_{ij}^{35}=I_3\int_0^L\varphi_i\varphi_j dx+\frac{4}{9h^2}I_7\int_0^L\varphi_{i,x}\varphi_{j,x}dx$$

$$M_{ij}^{44}=I_3\int_0^L\varphi_i\varphi_j dx+\frac{1}{4}I_5\int_0^L\varphi_{i,x}\varphi_{j,x}dx\,,\quad M_{ij}^{55}=I_5\int_0^L\varphi_i\varphi_j dx+\frac{1}{9}I_7\int_0^L\varphi_{i,x}\varphi_{j,x}dx$$

$$F_{0i}=\int_0^L q\varphi_i dx\,,\quad F_{1i}=-\frac{h}{2}\int_0^L q\varphi_i dx\,,\quad F_{2i}=\frac{h^2}{4}\int_0^L q\varphi_i dx \tag{17}$$

Finally, the static, vibration and buckling responses of composite beams can be determined by solving Eq. (16).

3. Numerical results

In this section, convergence and verification studies are carried out to demonstrate the accuracy of the present study. For static analysis, the beam is subjected to a uniformly distributed load with density q, applied on the surface $z=-h/2$ in the z-direction. Laminates are assumed to have equal thicknesses made of the same orthotropic materials whose properties are given in Table 3. For convenience, the following nondimensional terms are used:

$$\bar{w}=\frac{100w_0E_2bh^3}{qL^4},\quad \bar{\sigma}_x=\frac{bh^2}{qL^2}\sigma_x\left(\frac{L}{2},\frac{h}{2}\right),\quad \bar{\sigma}_z=\frac{b}{q}\sigma_z\left(\frac{L}{2},\frac{h}{2}\right),\quad \bar{\sigma}_{xz}=\frac{bh}{qL}\sigma_{xz}\left(0,0\right) \tag{18a}$$

$$\bar{N}_{cr}=\frac{N_{cr}L^2}{bE_2h^3} \tag{18b}$$

$$\bar{\omega}=\frac{\omega L^2}{h}\sqrt{\frac{\rho}{E_2}}\ \text{ for Material I (MAT I) and }\ \bar{\omega}=\frac{\omega L^2}{h}\sqrt{\frac{\rho}{E_1}}\ \text{ for MAT IV} \tag{18c}$$

The composite beams (MAT I, $0^0/90^0$, $L/h=5$, $E_1/E_2=40$) with different BCs are considered to evaluate the convergence. The nondimensional fundamental frequencies, critical buckling loads and mid-span displacements with respect to the series number m are given in Table 4. It can be seen that the present results converge at $m=12$ for the natural frequency and critical buckling load, and $m=14$ for the deflection. Thus, these converged numbers of series terms are chosen for the following analysis.

3.1. Example 1

The symmetric ($0^0/90^0/0^0$) and un-symmetric ($0^0/90^0$) beams with different L/h and BCs are considered in this example. The nondimensional fundamental frequencies, critical buckling loads and mid-span displacements ($x=L/2, z=0$) of beams are presented in Tables 5-7, respectively. The obtained results are compared with those from previous works using the HOBTs [14, 19, 21, 24-26, 30, 33] and the quasi-3D theories [15, 16, 22, 29]. It can be seen that the present results comply with earlier ones for both theories. It is also observed that there are differences between the results predicted by HOBT and quasi-3D theory, especially for un-symmetric and thick beams ($L/h=5$). For slender beams ($L/h=50$), however, the predictions between them are close to each other.

The nondimensional axial, transverse shear, and normal stresses of simply supported beams with $L/h=5,10,50$ are presented in Table 8, and also compared to the solutions obtained by Nguyen et al. [24] and Vo and Thai [31] using HOBT and Mantari and Canales [29] and Zenkour [15] using quasi-3D theory. Again, a good agreement with the previous models is found.

The effect of the ratio of material anisotropy (E_1/E_2) on nondimensional fundamental frequencies and critical buckling loads is plotted in Fig. 2. It indicates that the fundamental frequencies and critical buckling loads increase by the increase of E_1/E_2. The distribution of nondimensional transverse displacements through the thickness for $L/h = 5, 10, 50$ is displayed in Figs. 3-5. It is observed that the nonlinear variation of the transverse displacement is clearly displayed for thick beams ($L/h = 5$) with all BCs.

3.2. Example 2

The ($0^0/\theta/0^0$) and ($0^0/\theta$) beams, which are extended from previous example, are considered. Tables 9-12 present the variation of nondimensional fundamental frequencies, critical buckling loads, mid-span displacements ($x = L/2, z = 0$) and stresses of beams with respect to the fiber angle. It can be seen that the present results in Tables 11 and 12 are close with those of Vo et al. [28], which used a quasi-3D theory. Figs. 6-8 show the variation of displacements for very thick beams ($L/h = 3$) with the increase of fiber angle θ. It is observed that there are significant differences between the results of HOBT and quasi-3D solutions. The distribution of nondimensional shear and axial stresses through the thickness of ($0^0/60^0/0^0$) and ($0^0/60^0$) beams is displayed in Figs. 9 and 10. It can be seen that the shear stress at top and bottom surface is vanished as expected.

3.3. Example 3

This example aims to analyze the behaviors of composite beams with arbitrary lay-ups. The symmetric single-layered C-F beams with fiber angles 15^0 and 30^0 (MAT III) are first considered. The first five natural frequencies are displayed in Table 13 and compared with those from Chen et al. [17] and experiment results of Abarcar and Cunniff [42]. It is seen that there is consistency between present results and those from [17] and [42], especially for the first mode of vibration. Next, the un-symmetric (45^0/-45^0/45^0/-45^0) and (30^0/-50^0/50^0/-30^0) beams (MAT IV) with various BCs are considered. The responses on fundamental frequencies are reported in Table 14. Good agreements between the present theory and previous studies are again found. Finally, the symmetric $(\theta/-\theta)_s$ composite beams (MAT IV) are considered. The effects of fiber angle on the natural frequencies, critical buckling loads and displacements are illustrated in Table 15. In addition, the nondimensional fundamental frequencies are also shown in Fig. 11. It can be seen that the present natural frequencies are closer than to those of [17, 20] and smaller than to those of [6, 24] which neglected the Poisson's effect, especially for $10^0 \le \theta \le 60^0$. This phenomenon can be explained by the fact that Poisson's effect is incorporated in the constitutive equations by assuming $\sigma_y = \sigma_{xy} = \sigma_{yz} = 0$. It means that the strains (ε_y, γ_{yz}, γ_{xy}) are nonzero and this causes the beams more flexible [18]. This indicated that the Poisson's effect is quite significant to composite beams with arbitrary lay-ups, and neglecting this effect is only suitable for the cross-ply composite beams [38]. There is a deviation between the present critical buckling load and those from Wang et al. [38], especially for the fiber angles $15^0, 30^0$ and 45^0. It can be explained partly by the difference in the displacement fields between present study and Wang et al. [38], which considered the first-order variation for both x- and y-directions (FOBT). For this reason, bending-torsion coupling effect occurred in Wang et al. [38]. This effect depended on the fiber angle of composite lay-up. For example, Teh and Huang [27] stated that this maximum coupling effect varies from fiber angle from 24^0 to 25^0 of cantilever graphite/epoxy beams. This study as well as most of previous research reviewed in Ref. [1] ignored this bending-torsion coupling effect for rectangular composite beams. This is the main reason for the difference between the obtained critical buckling loads and those of Wang et al. [38].

4. Conclusions

The new shape functions, which combined polynomial and exponential functions, are presented to study the static, buckling and free vibration behaviors of laminated composite beams with arbitrary lay-ups. The displacement field is based on a quasi-3D theory accounting for a higher-order variation of both axial and transverse displacements. Poisson's effect is incorporated in beam model. Numerical results for different BCs are obtained to compare with previous studies and investigate effects of material anisotropy, Poisson's ratio and fiber angles on the natural frequencies, buckling loads, displacements and stresses of composite beams. The obtained results show that the normal strain effects are significant for un-symmetric and thick beams. The Poisson's effect is also important for composite beams with arbitrary lay-ups, and thus omitting this effect is only suitable for the cross-ply ones. The present model is found to be appropriate for the bending, buckling and vibration analysis of composite beams.

Acknowledgements

This research is funded by Vietnam National Foundation for Science and Technology Development (NAFOSTED) under Grant No. 107.02-2015.07.

References

1. Sayyad A.S. and Ghugal Y.M., *Bending, buckling and free vibration of laminated composite and sandwich beams: A critical review of literature.* Composite Structures, 2017.
2. Bernoulli J., *Curvatura laminae elasticae.* Acta eruditorum. **1694**(13): p. 262-276.
3. Ebrahimi M., Moeinfar A., and Shakeri M., *Nonlinear Free Vibration of Hybrid Composite Moving Beams Embedded with Shape Memory Alloy Fibers.* International Journal of Structural Stability and Dynamics, 2016. **16**(07): p.

1550032.

4. Timoshenko S.P., *LXVI. On the correction for shear of the differential equation for transverse vibrations of prismatic bars.* The London, Edinburgh, and Dublin Philosophical Magazine and Journal of Science, 1921. **41**(245): p. 744-746.
5. Timoshenko S.P., *X. On the transverse vibrations of bars of uniform cross-section.* The London, Edinburgh, and Dublin Philosophical Magazine and Journal of Science, 1922. **43**(253): p. 125-131.
6. Chandrashekhara K., Krishnamurthy K., and Roy S., *Free vibration of composite beams including rotary inertia and shear deformation.* Composite Structures, 1990. **14**(4): p. 269-279.
7. Komijani M., Reddy J., Eslami M., and Bateni M., *An analytical approach for thermal stability analysis of two-layer Timoshenko beams.* International Journal of Structural Stability and Dynamics, 2013. **13**(08): p. 1350036.
8. Chen W.-R. and Chang H., *Vibration analysis of functionally graded Timoshenko beams.* International Journal of Structural Stability and Dynamics, 2018: p. 1850007.
9. Santiuste C., Sánchez-Sáez S., and Barbero E., *Dynamic analysis of bending–torsion coupled composite beams using the Flexibility Influence Function Method.* International Journal of Mechanical Sciences, 2008. **50**(12): p. 1611-1618.
10. Levinson M., *A new rectangular beam theory.* Journal of Sound and vibration, 1981. **74**(1): p. 81-87.
11. Krishna Murty A., *Toward a consistent beam theory.* AIAA journal, 1984. **22**(6): p. 811-816.
12. Reddy J.N., *A simple higher-order theory for laminated composite plates.* Journal

of applied mechanics, 1984. **51**(4): p. 745-752.

13. Ghugal Y. and Shimpi R. *A trigonometric shear deformation theory for flexure and free vibration of isotropic thick beams*. in *Structural Engineering Convention, SEC-2000, IIT Bombay, India*. 2000.
14. Khdeir A. and Reddy J., *An exact solution for the bending of thin and thick cross-ply laminated beams.* Composite Structures, 1997. **37**(2): p. 195-203.
15. Zenkour A.M., *Transverse shear and normal deformation theory for bending analysis of laminated and sandwich elastic beams.* Mechanics of Composite Materials and Structures, 1999. **6**(3): p. 267-283.
16. Matsunaga H., *Vibration and buckling of multilayered composite beams according to higher order deformation theories.* Journal of Sound and Vibration, 2001. **246**(1): p. 47-62.
17. Chen W., Lv C., and Bian Z., *Free vibration analysis of generally laminated beams via state-space-based differential quadrature.* Composite Structures, 2004. **63**(3): p. 417-425.
18. Li J., Huo Q., Li X., Kong X., and Wu W., *Vibration analyses of laminated composite beams using refined higher-order shear deformation theory.* International Journal of Mechanics and Materials in Design, 2014. **10**(1): p. 43-52.
19. Aydogdu M., *Buckling analysis of cross-ply laminated beams with general boundary conditions by Ritz method.* Composites Science and Technology, 2006. **66**(10): p. 1248-1255.
20. Aydogdu M., *Free vibration analysis of angle-ply laminated beams with general boundary conditions.* Journal of reinforced plastics and composites, 2006. **25**(15): p. 1571-1583.

21. Aydogdu M., *Vibration analysis of cross-ply laminated beams with general boundary conditions by Ritz method.* International Journal of Mechanical Sciences, 2005. **47**(11): p. 1740-1755.

22. Mantari J. and Canales F., *Free vibration and buckling of laminated beams via hybrid Ritz solution for various penalized boundary conditions.* Composite Structures, 2016. **152**: p. 306-315.

23. Canales F. and Mantari J., *Buckling and free vibration of laminated beams with arbitrary boundary conditions using a refined HSDT.* Composites Part B: Engineering, 2016. **100**: p. 136-145.

24. Nguyen T.-K., Nguyen N.-D., Vo T.P., and Thai H.-T., *Trigonometric-series solution for analysis of laminated composite beams.* Composite Structures, 2017. **160**: p. 142-151.

25. Khdeir A.A. and Redd J.N., *Buckling of cross-ply laminated beams with arbitrary boundary conditions.* Composite Structures, 1997. **37**(1): p. 1-3.

26. Khdeir A.A. and Reddy J.N., *Free vibration of cross-ply laminated beams with arbitrary boundary conditions.* International Journal of Engineering Science, 1994. **32**(12): p. 1971-1980.

27. Teh K. and Huang C., *The effects of fibre orientation on free vibrations of composite beams.* Journal of Sound and Vibration, 1980. **69**(2): p. 327-337.

28. Vo T.P., Thai H.-T., Nguyen T.-K., Lanc D., and Karamanli A., *Flexural analysis of laminated composite and sandwich beams using a four-unknown shear and normal deformation theory.* Composite Structures, 2017.

29. Mantari J. and Canales F., *Finite element formulation of laminated beams with capability to model the thickness expansion.* Composites Part B: Engineering, 2016.

101: p. 107-115.

30. Vo T.P. and Thai H.-T., *Vibration and buckling of composite beams using refined shear deformation theory.* International Journal of Mechanical Sciences, 2012. **62**(1): p. 67-76.
31. Vo T.P. and Thai H.-T., *Static behavior of composite beams using various refined shear deformation theories.* Composite Structures, 2012. **94**(8): p. 2513-2522.
32. Vidal P. and Polit O., *A family of sinus finite elements for the analysis of rectangular laminated beams.* Composite Structures, 2008. **84**(1): p. 56-72.
33. Murthy M., Mahapatra D.R., Badarinarayana K., and Gopalakrishnan S., *A refined higher order finite element for asymmetric composite beams.* Composite Structures, 2005. **67**(1): p. 27-35.
34. Shi G. and Lam K., *Finite element vibration analysis of composite beams based on higher-order beam theory.* Journal of Sound and Vibration, 1999. **219**(4): p. 707-721.
35. Marur S. and Kant T., *Free vibration analysis of fiber reinforced composite beams using higher order theories and finite element modelling.* Journal of Sound and Vibration, 1996. **194**(3): p. 337-351.
36. Chandrashekhara K. and Bangera K.M., *Free vibration of composite beams using a refined shear flexible beam element.* Computers & structures, 1992. **43**(4): p. 719-727.
37. Filippi M. and Carrera E., *Bending and vibrations analyses of laminated beams by using a zig-zag-layer-wise theory.* Composites Part B: Engineering, 2016. **98**: p. 269-280.
38. Wang X., Zhu X., and Hu P., *Isogeometric finite element method for buckling*

analysis of generally laminated composite beams with different boundary conditions. International Journal of Mechanical Sciences, 2015. **104**: p. 190-199.

39. Jun L., Xiaobin L., and Hongxing H., *Free vibration analysis of third-order shear deformable composite beams using dynamic stiffness method.* Archive of Applied Mechanics, 2009. **79**(12): p. 1083-1098.
40. Shao D., Hu S., Wang Q., and Pang F., *Free vibration of refined higher-order shear deformation composite laminated beams with general boundary conditions.* Composites Part B: Engineering, 2017. **108**: p. 75-90.
41. Reddy J.N., *Mechanics of laminated composite plates: theory and analysis*. 1997: CRC press.
42. Abarcar R.B. and Cunniff P.F., *The vibration of cantilever beams of fiber reinforced material.* Journal of Composite Materials, 1972. **6**(3): p. 504-517.

FIGURE CAPTIONS

Figure 1. Geometry and coordinate of a laminated composite beam.

Figure 2. Effects of material anisotropy on the nondimensional fundamental frequencies and critical buckling loads of ($0^0/90^0$) and ($0^0/90^0/0^0$) S-S composite beams

Figure 3. Distribution of nondimensional transverse displacement through the thickness of ($0^0/90^0$) and ($0^0/90^0/0^0$) S-S composite beams (MAT II).

Figure 4. Distribution of nondimensional transverse displacement through the thickness of ($0^0/90^0$) and ($0^0/90^0/0^0$) C-F composite beams MAT II).

Figure 5. Distribution of nondimensional transverse displacement through the thickness of ($0^0/90^0$) and ($0^0/90^0/0^0$) C-C composite beams (MAT II).

Figure 6. The nondimensional mid-span transverse displacement with respect to the fiber angle change of S-S composite beams ($L/h=3$, MAT II).

Figure 7. The nondimensional mid-span transverse displacement with respect to the fiber angle change of C-F composite beams ($L/h=3$, MAT II).

Figure 8. The nondimensional mid-span transverse displacement with respect to the fiber angle change of C-C composite beams ($L/h=3$, MAT II).

Figure 9. Distribution of nondimensional stresses through the thickness of ($0^0/60^0/0^0$)

Figure 10. Distribution of nondimensional stresses through the thickness of

Figure 11. Effects of the fiber angle change on the nondimensional fundamental frequency of $(\theta/-\theta)_s$ composite beams with various BCs (MAT IV).

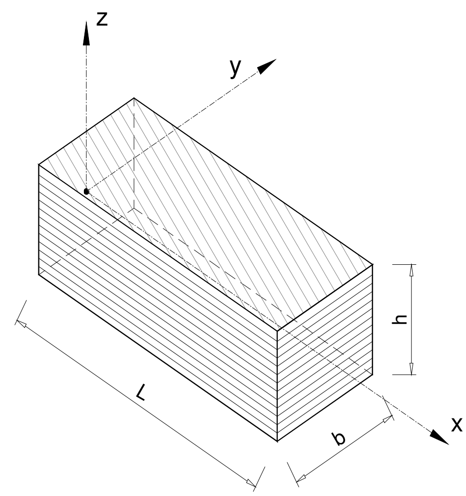

Figure 1. Geometry and coordinate of a laminated composite beam.

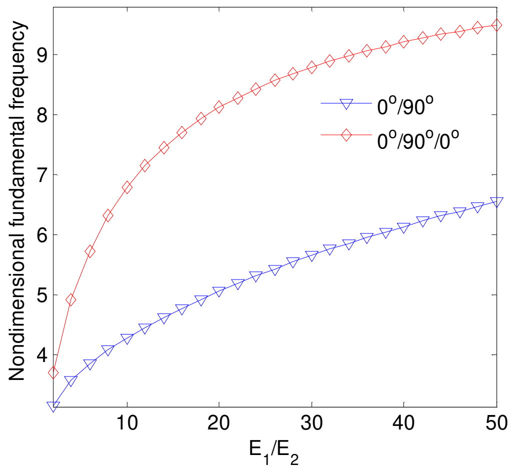

a. Fundamental frequency

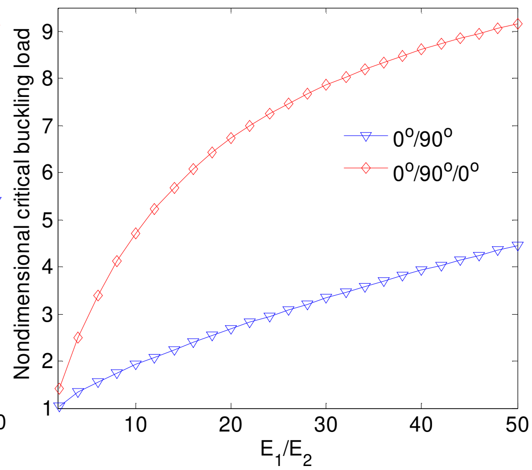

b. Critical buckling load

Figure 2. Effects of material anisotropy on the nondimensional fundamental frequencies and critical buckling loads of ($0^0/90^0$) and ($0^0/90^0/0^0$) S-S composite beams. (*L/h*=5, MAT I).

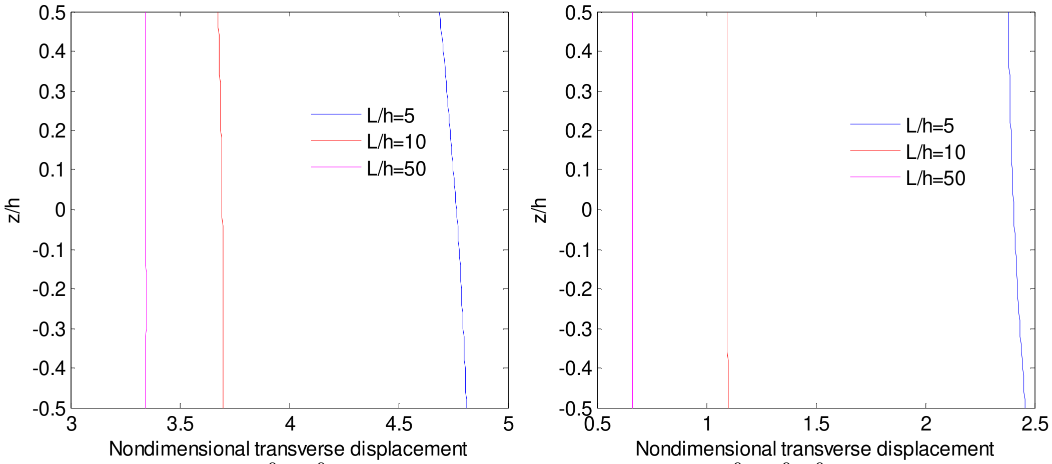

a. $0^0/90^0$ b. $0^0/90^0/0^0$

Figure 3. Distribution of nondimensional transverse displacement through the thickness of ($0^0/90^0$) and ($0^0/90^0/0^0$) S-S composite beams (MAT II).

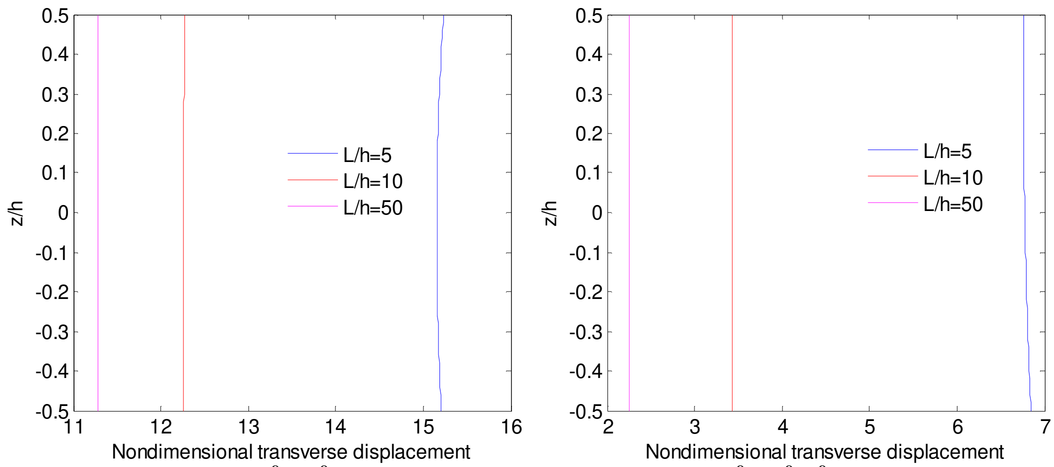

a. $0^0/90^0$ b. $0^0/90^0/0^0$

Figure 4. Distribution of nondimensional transverse displacement through the thickness of ($0^0/90^0$) and ($0^0/90^0/0^0$) C-F composite beams (MAT II).

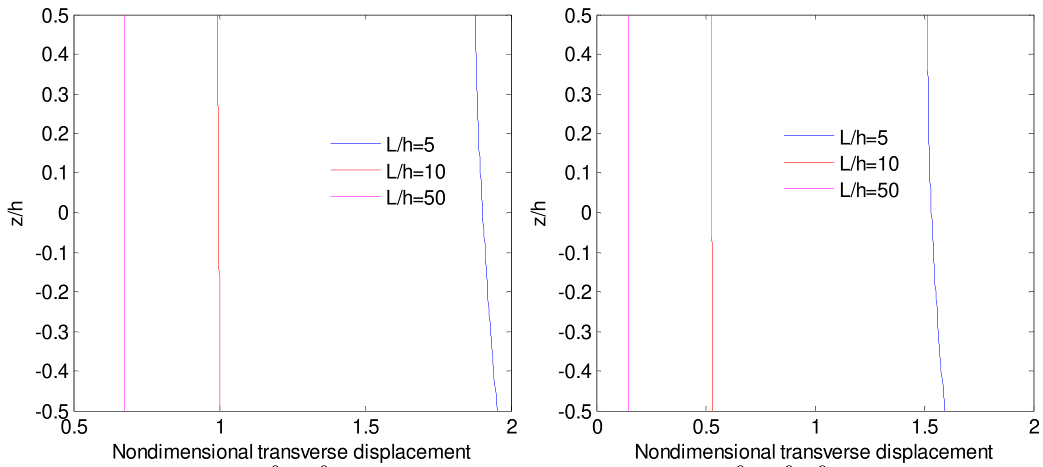

a. $0^0/90^0$ b. $0^0/90^0/0^0$

Figure 5. Distribution of nondimensional transverse displacement through the thickness of ($0^0/90^0$) and ($0^0/90^0/0^0$) C-C composite beams (MAT II).

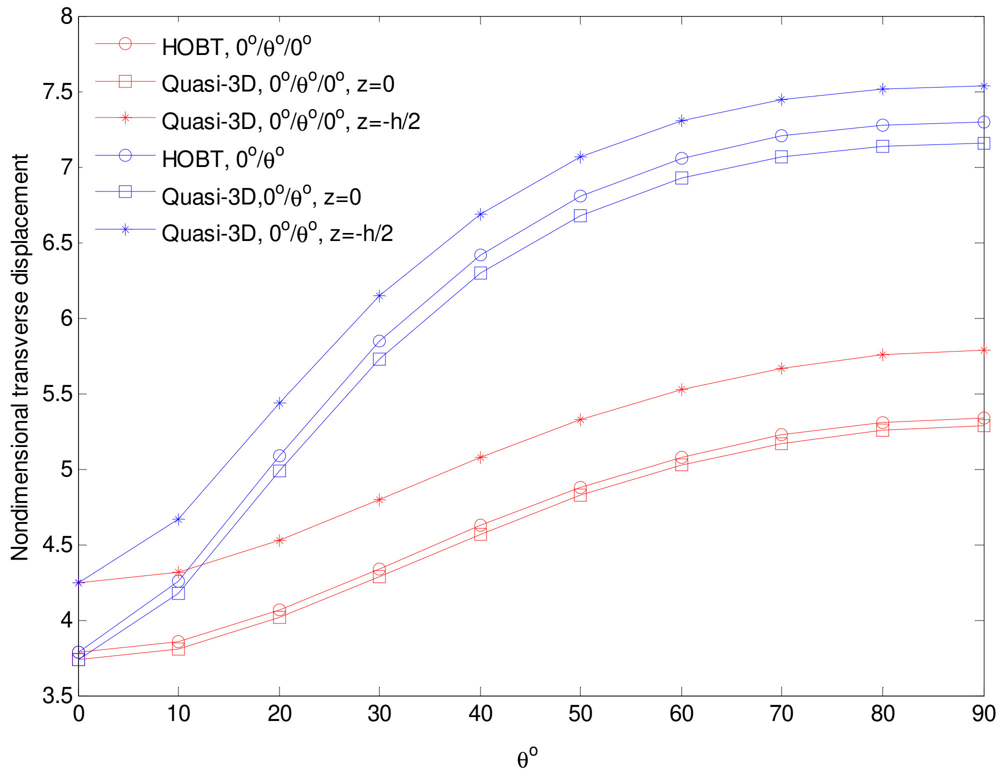

Figure 6. The nondimensional mid-span transverse displacement with respect to the fiber angle change of S-S composite beams ($L/h=3$, MAT II).

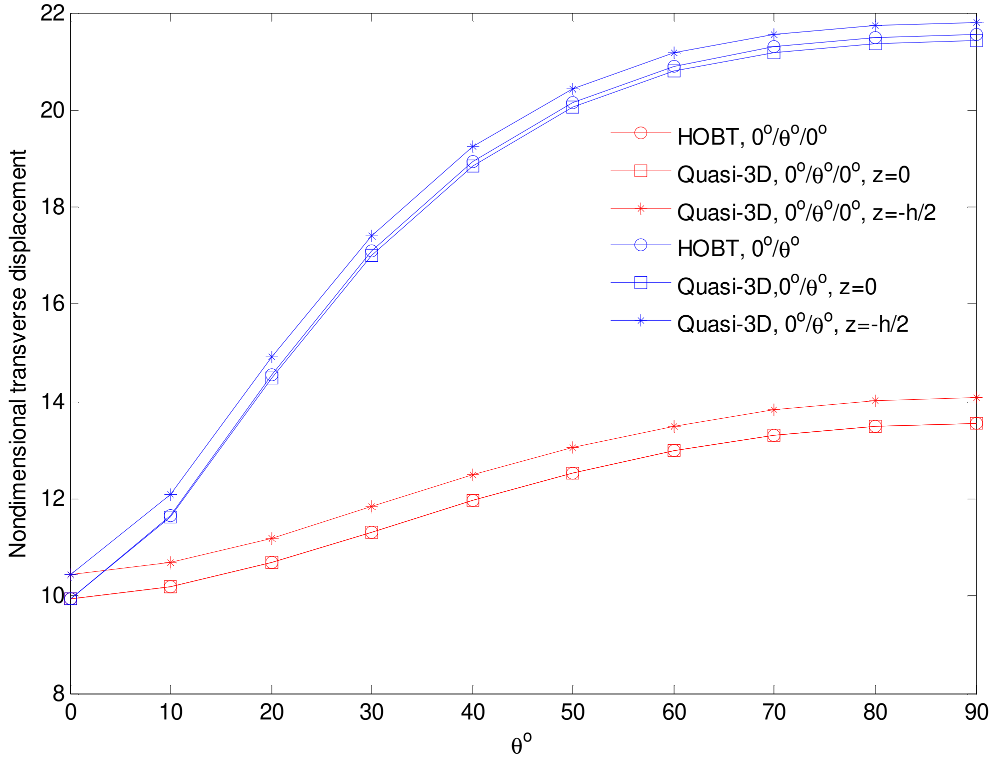

Figure 7. The nondimensional mid-span transverse displacement with respect to the fiber angle change of C-F composite beams ($L/h=3$, MAT II).

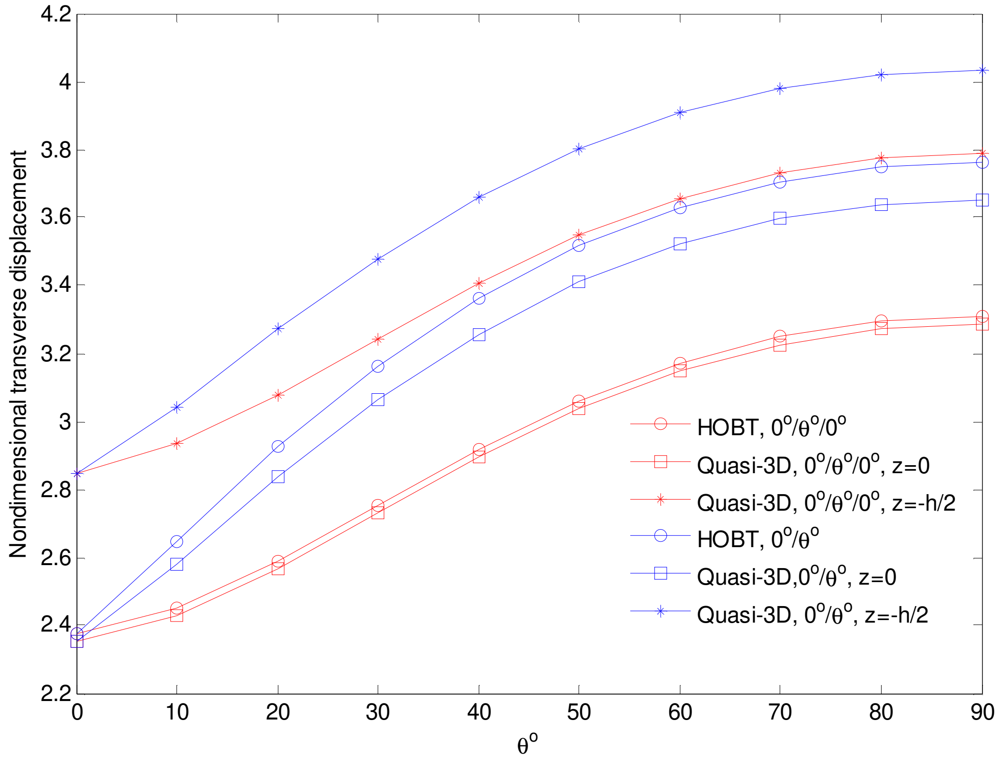

Figure 8. The nondimensional mid-span transverse displacement with respect to the fiber angle change of C-C composite beams ($L/h = 3$, MAT II).

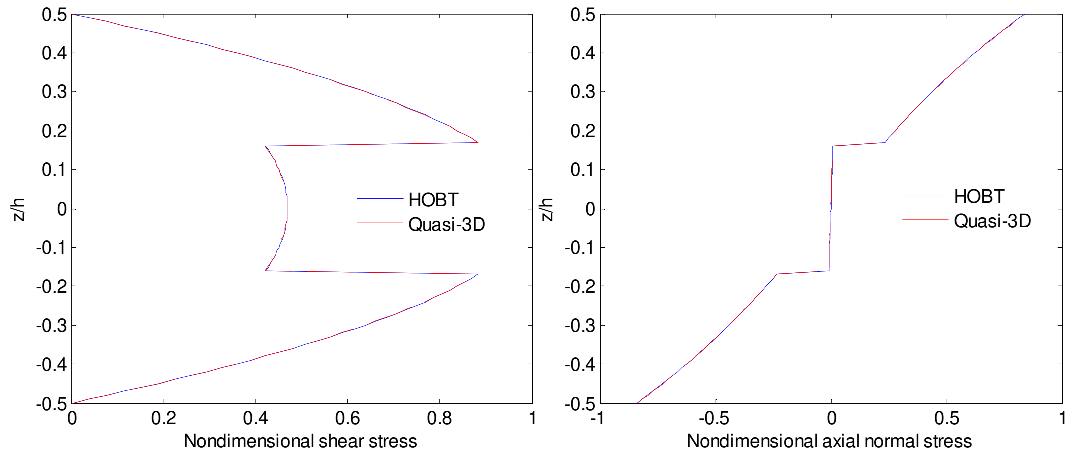

a. σ_{xz} b. σ_{xx}

Figure 9. Distribution of nondimensional stresses through the thickness of ($0^0/60^0/0^0$) S-S composite beams ($L/h=10$, MAT II).

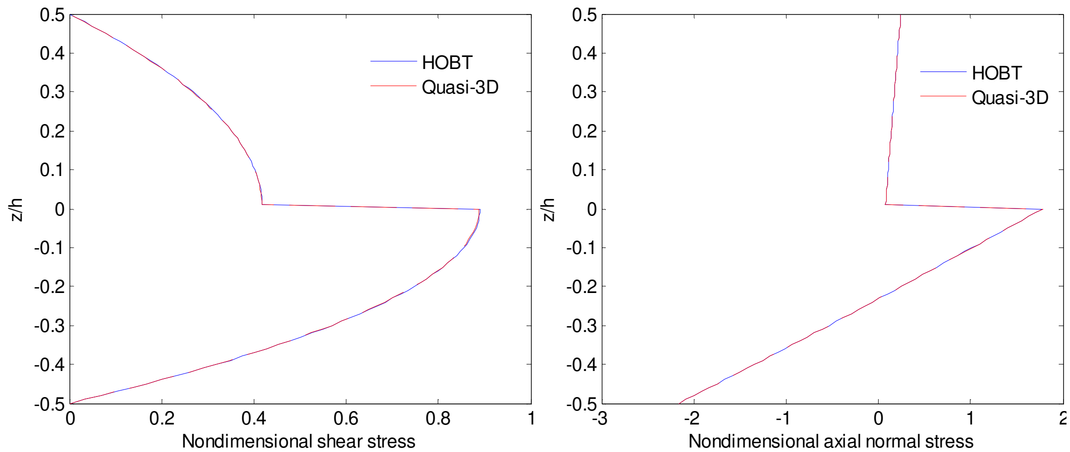

a. σ_{xz} b. σ_{xx}

Figure 10. Distribution of nondimensional stresses through the thickness of ($0^0/60^0$) S-S composite beams ($L/h=10$, MAT II).

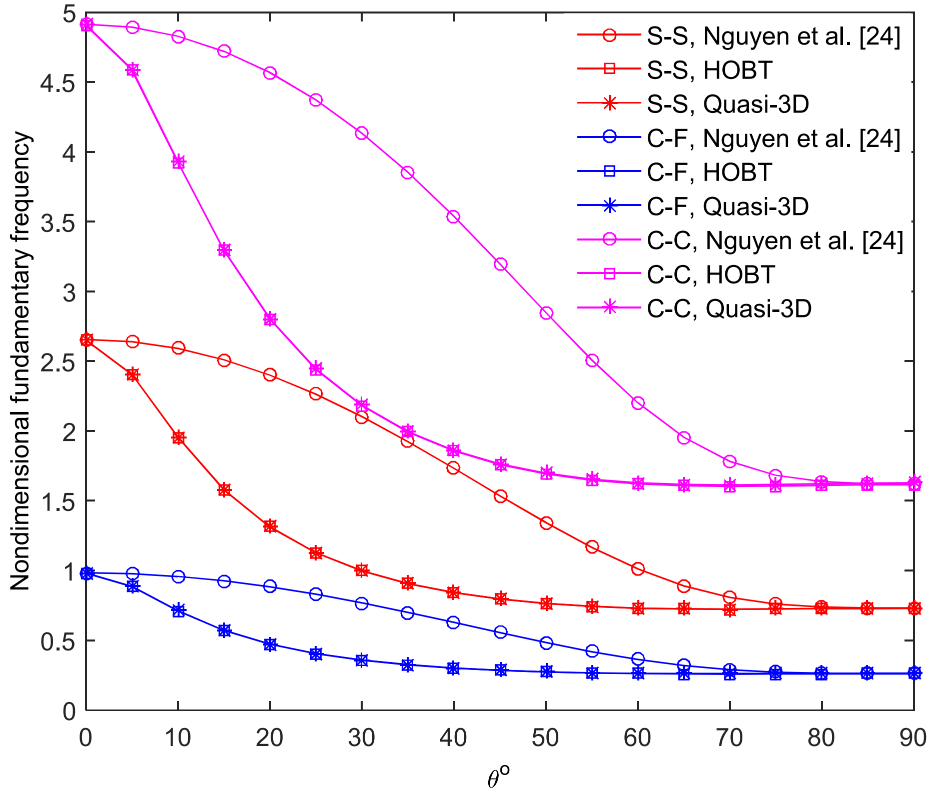

Figure 11. Effects of the fiber angle change on the nondimensional fundamental frequency of $(\theta/-\theta)_s$ composite beams with various BCs (MAT IV).

TABLE CAPTIONS

Table 1. Shape functions.

Table 2. Kinematic BCs.

Table 3. Material properties of laminated composite beams.

Table 4. Convergence studies for the nondimensional fundamental frequencies, critical buckling loads and mid-span displacements of ($0^0/90^0$) composite beams (MAT I, $L/h=5$, $E_1/E_2=40$).

Table 5. Nondimensional fundamental frequencies of ($0^0/90^0/0^0$) and ($0^0/90^0$) composite beams (MAT I, $E_1/E_2=40$).

Table 6. Nondimensional critical buckling loads of ($0^0/90^0/0^0$) and ($0^0/90^0$) composite beams (MAT I, $E_1/E_2=40$).

Table 7. Nondimensional mid-span displacements of ($0^0/90^0/0^0$) and ($0^0/90^0$) composite beams under a uniformly distributed load (MAT II).

Table 8. Nondimensional stresses of ($0^0/90^0/0^0$) and ($0^0/90^0$) S-S composite beams

Table 9. Nondimensional fundamental frequencies of ($0^0/\theta/0^0$) and ($0^0/\theta$) composite beams (MAT I, $E_1/E_2=40$).

Table 10. Nondimensional critical buckling loads of ($0^0/\theta/0^0$) and ($0^0/\theta$) composite beams (MAT I, $E_1/E_2=40$).

Table 11. Nondimensional mid-span displacements of ($0^0/\theta/0^0$) and ($0^0/\theta$) composite beams under a uniformly distributed load (MAT II).

Table 12. Nondimensional stresses of ($0^0/\theta/0^0$) and ($0^0/\theta$) S-S composite beams under a uniformly distributed load (MAT II).

Table 13. Fundamental frequencies (Hz) of single-layer C-F composite beam (MAT III).

Table 14. Nondimensional fundamental frequencies of composite beams (MAT IV).

Table 15. Nondimensional fundamental frequencies, critical buckling loads and mid-span displacements of $\left(\theta/-\theta\right)_s$ composite beams (MAT IV).

Table 1. Shape functions.

BC	$\varphi_j(x)$
S-S	$x\left(L-x\right)e^{\frac{x}{jL}}$
C-F	$x^2 e^{\frac{x}{jL}}$
C-C	$x^2\left(L-x\right)^2 e^{\frac{x}{jL}}$

Table 2. Kinematic BCs.

BC	Position	Value
S-S	x=0	$w_0 = 0$, $w_1 = 0$, $w_2 = 0$
	x=L	$w_0 = 0$, $w_1 = 0$, $w_2 = 0$
C-F	x=0	$u_0 = 0$, $u_1 = 0$, $w_0 = 0$, $w_1 = 0$, $w_2 = 0$, $w_{0.x} = 0$, $w_{1.x} = 0$, $w_{2.x} = 0$
	x=L	
C-C	x=0	$u_0 = 0$, $u_1 = 0$, $w_0 = 0$, $w_1 = 0$, $w_2 = 0$, $w_{0.x} = 0$, $w_{1.x} = 0$, $w_{2.x} = 0$
	x=L	$u_0 = 0$, $u_1 = 0$, $w_0 = 0$, $w_1 = 0$, $w_2 = 0$, $w_{0,x} = 0$, $w_{1,x} = 0$, $w_{2,x} = 0$

Table 3. Material properties of laminated composite beams.

Material properties	MAT I [21]	MAT II [14]	MAT III [17, 42]	MAT IV [6]
E_1 (GPa)	E_1/E_2=open	E_1/E_2=25	129.11	144.8
$E_2=E_3$(GPa)	-	-	9.408	9.65
$G_{12}=G_{13}$ (GPa)	$0.6E_2$	$0.5E_2$	5.1568	4.14
G_{23} (GPa)	$0.5E_2$	$0.2E_2$	3.45	3.45
$\nu_{12}=\nu_{13}=\nu_{23}$	0.25	0.25	0.3	0.3
ρ (kg/m^3)	-	-	1550.1	-
L (m)	L/h=open	L/h=open	0.1905	L/h=15
h (m)	-	-	0.003175	-
b (m)	-	-	0.0127	-

Table 4. Convergence studies for the nondimensional fundamental frequencies, critical buckling loads and mid-span displacements of ($0^0/90^0$) composite beams (MAT I, $L/h=5$, $E_1/E_2=40$).

BC	m						
	2	4	6	8	10	12	14
a. Fundamental frequency							
S-S	6.3764	6.1406	6.1400	6.1400	6.1400	6.1400	6.1400
C-F	2.5879	2.3927	2.3845	2.3824	2.3820	2.3819	2.3819
C-C	10.3078	10.0566	9.9881	9.9650	9.9519	9.9435	9.9382
b. Critical buckling load							
S-S	4.1943	3.9217	3.9211	3.9211	3.9211	3.9211	3.9211
C-F	1.2668	1.2365	1.2341	1.2334	1.2333	1.2333	1.2333
C-C	8.8169	8.6247	8.6167	8.6160	8.6156	8.6154	8.6153
c. Deflection							
S-S	3.0041	3.2540	3.2481	3.2490	3.2488	3.2488	3.2488
C-F	6.9948	10.3704	10.4354	10.5022	10.4986	10.5079	10.5056
C-C	1.1999	1.2008	1.2440	1.2369	1.2473	1.2442	1.2455

Table 5. Nondimensional fundamental frequencies of ($0^0/90^0/0^0$) and ($0^0/90^0$) composite beams (MAT I, $E_1 / E_2 = 40$).

Theory	Reference	$0^0/90^0/0^0$			$0^0/90^0$		
		L/h=5	10	50	*L/h*=5	10	50
a. S-S beams							
HOBT	Present	9.206	13.607	17.449	6.125	6.940	7.297
	Nguyen et al. [24]	9.208	13.614	17.462	6.128	6.945	7.302
	Khdeir and Reddy [26]	9.208	13.614	-	6.128	6.945	-
	Vo and Thai [30]	9.206	13.607	17.449	6.058	6.909	7.296
	Murthy et al. [33]	9.207	13.611	-	6.045	6.908	-
	Aydogdu [21]	9.207	-	-	6.144	-	-
Quasi-3D	Present	9.208	13.610	17.449	6.140	6.948	7.297
	Mantari and Canales [22]	9.208	13.610	-	6.109	6.913	-
	Matsunaga [16]	9.200	13.608	-	5.662	6.756	-
b. C-F beams							
HOBT	Present	4.230	5.490	6.262	2.381	2.541	2.603
	Nguyen et al. [24]	4.234	5.498	6.267	2.383	2.543	2.605
	Khdeir and Reddy [26]	4.234	5.495	-	2.386	2.544	-
	Murthy et al. [33]	4.230	5.491	-	2.378	2.541	-
	Aydogdu [21]	4.234	-	-	2.384	-	-
Quasi-3D	Present	4.223	5.491	6.262	2.382	2.543	2.604
	Mantari and Canales [22]	4.221	5.490	-	2.375	2.532	-
c. C-C beams							
HOBT	Present	11.601	19.707	37.629	10.019	13.653	16.414
	Nguyen et al. [24]	11.607	19.728	37.679	10.027	13.670	16.429
	Khdeir and Reddy [26]	11.603	19.712	-	10.026	13.660	-
	Murthy et al. [33]	11.602	19.719	-	10.011	13.657	-
	Aydogdu [21]	11.637	-	-	10.103	-	-
Quasi-3D	Present	11.499	19.672	37.633	9.944	13.664	16.432
	Mantari and Canales [22]	11.486	19.652	-	9.974	13.628	-

Table 6. Nondimensional critical buckling loads of ($0^0/90^0/0^0$) and ($0^0/90^0$) composite beams (MAT I, $E_1 / E_2 = 40$).

Theory	Reference	$0^0 / 90^0 / 0^0$			$0^0 / 90^0$		
		L/*h*=5	10	50	*L*/*h*=5	10	50
a. S-S beams							
HOBT	Present	8.609	18.814	30.859	3.902	4.935	5.398
	Nguyen et al. [24]	8.613	18.832	30.906	3.907	4.942	5.406
	Khdeir and Reddy [25]	8.613	18.832	-	-	-	-
	Aydogdu [19]	8.613	-	-	3.906	-	-
Quasi-3D	Present	8.613	18.822	30.860	3.921	4.946	5.398
	Mantari and Canales [22]	8.585	18.796	-	3.856	4.887	-
b. C-F beams							
HOBT	Present	4.704	6.763	7.873	1.234	1.322	1.353
	Nguyen et al. [24]	4.708	6.772	7.886	1.236	1.324	1.356
	Khdeir and Reddy [25]	4.708	6.772	-	-	-	-
	Aydogdu [19]	4.708	-	-	1.236	-	-
Quasi-3D	Present	4.699	6.762	7.874	1.233	1.324	1.354
	Mantari and Canales [22]	4.673	6.757	-	1.221	1.311	-
c. C-C beams							
HOBT	Present	11.648	34.437	114.237	8.668	15.609	21.339
	Nguyen et al. [24]	11.652	34.453	114.398	8.674	15.626	21.372
	Khdeir and Reddy [25]	11.652	34.453	-	-	-	-
Quasi-3D	Present	11.652	34.452	114.260	8.615	15.693	21.371
	Mantari and Canales [22]	11.502	34.365	-	8.509	15.468	-

Table 7. Nondimensional mid-span displacements of ($0^0/90^0/0^0$) and ($0^0/90^0$) composite beams under a uniformly distributed load (MAT II).

Theory	Reference	0^0 / 90^0 / 0^0			0^0 / 90^0		
		L/*h*=5	10	50	*L*/*h*=5	10	50
a. S-S beams							
HOBT	Present	2.414	1.098	0.666	4.785	3.697	3.345
	Nguyen et al. [24]	2.412	1.096	0.665	4.777	3.688	3.336
	Murthy et al. [33]	2.398	1.090	0.661	4.750	3.668	3.318
	Khdeir and Reddy [14]	2.412	1.096	0.666	4.777	3.688	3.336
Quasi-3D	Present	2.405	1.097	0.666	4.764	3.694	3.345
	Zenkour [15]	2.405	1.097	0.666	4.828	3.763	3.415
	Mantari and Canales [29]	-	1.097	-	-	3.731	-
b. C-F beams							
HOBT	Present	6.830	3.461	2.257	15.308	12.371	11.365
	Nguyen et al. [24]	6.813	3.447	2.250	15.260	12.330	11.335
	Murthy et al. [33]	6.836	3.466	2.262	15.334	12.398	11.392
	Khdeir and Reddy [14]	6.824	3.455	2.251	15.279	12.343	11.337
Quasi-3D	Present	6.844	3.451	2.256	15.260	12.339	11.343
	Mantari and Canales [29]	-	3.459	-	-	12.475	-
c. C-C beams							
HOBT	Present	1.538	0.532	0.147	1.924	1.007	0.680
	Nguyen et al. [24]	1.536	0.531	0.147	1.920	1.004	0.679
	Khdeir and Reddy [14]	1.537	0.532	0.147	1.922	1.005	0.679
Quasi-3D	Present	1.543	0.532	0.147	1.916	1.005	0.679
	Mantari and Canales [29]	-	0.532	-	-	1.010	-

Table 8. Nondimensional stresses of ($0^0/90^0/0^0$) and ($0^0/90^0$) S-S composite beams under a uniformly distributed load (MAT II).

Theory	Reference	$0^0/90^0/0^0$			$0^0/90^0$		
		L/*h*=5	10	50	*L*/*h*=5	10	50
a. Normal axial stress							
HOBT	Present	1.0669	0.8500	0.8705	0.2361	0.2342	0.2336
	Nguyen et al. [24]	1.0696	0.8516	-	0.2362	0.2343	-
	Zenkour [15]	1.0669	0.8500	0.7805	0.2362	0.2343	0.2336
	Vo and Thai [31]	1.0670	0.8503	-	0.2361	0.2342	-
Quasi-3D	Present	1.0732	0.8504	0.7806	0.2380	0.2346	0.2336
	Zenkour [15]	1.0732	0.8506	0.7806	0.2276	0.2246	0.2236
	Mantari and Canales [29]	-	0.8501	-	-	0.2227	-
b. Shear stress							
HOBT	Present	0.4057	0.4311	0.4523	0.9205	0.9565	0.9878
	Nguyen et al. [24]	0.4050	0.4289	-	0.9174	0.9483	-
	Zenkour [15]	0.4057	0.4311	0.4514	0.9211	0.9572	0.9860
	Vo and Thai [31]	0.4057	0.4311	-	0.9187	0.9484	-
Quasi-3D	Present	0.4013	0.4286	0.4521	0.9052	0.9476	0.9869
	Zenkour [15]	0.4013	0.4289	0.4509	0.9038	0.9469	0.9814
	Mantari and Canales [29]	-	-	-	-	0.9503	-
c. Transverse normal stress							
Quasi-3D	Present	0.1833	0.1787	0.1804	0.2966	0.2911	0.3046
	Zenkour [15]	0.1833	0.1803	0.1804	0.2988	0.2982	0.2983

Table 9. Nondimensional fundamental frequencies of ($0^0/\theta/0^0$) and ($0^0/\theta$) composite beams (MAT I, $E_1/E_2 = 40$).

Lay-up	BC	*L/h*	Fiber angle (θ)						
			0^0	15^0	30^0	45^0	60^0	75^0	90^0
$0^0/\theta/0^0$	S-S	5	9.5498	9.5165	9.4487	9.3630	9.2831	9.2279	9.2083
		10	13.9976	13.8822	13.8130	13.7400	13.6729	13.6264	13.6099
		50	17.7844	17.5246	17.4788	17.4642	17.4558	17.4509	17.4493
	C-F	5	4.3628	4.3307	4.3047	4.2754	4.2484	4.2297	4.2231
		10	5.6259	5.5622	5.5403	5.5220	5.5059	5.4948	5.4909
		50	6.3803	6.2856	6.2697	6.2655	6.2635	6.2625	6.2622
	C-C	5	12.0240	11.9365	11.8341	11.7130	11.6020	11.5260	11.4992
		10	20.4355	20.3428	20.1923	20.0062	19.8335	19.7144	19.6723
		50	38.4410	37.9379	37.8172	37.7449	37.6863	37.6471	37.6333
$0^0/\theta$	S-S	5	9.5498	7.9829	6.8336	6.3948	6.2215	6.1561	6.1400
		10	13.9976	10.0656	7.9772	7.3028	7.0561	6.9682	6.9475
		50	17.7844	11.2187	8.5069	7.7036	7.4191	7.3199	7.2971
	C-F	5	4.3628	3.3266	2.7077	2.4964	2.4173	2.3887	2.3819
		10	5.6259	3.7996	2.9428	2.6785	2.5837	2.5505	2.5428
		50	6.3803	4.0080	3.0359	2.7488	2.6474	2.6123	2.6043
	C-C	5	12.0240	11.0882	10.4823	10.1844	10.0347	9.9640	9.9435
		10	20.4355	17.3592	15.0934	14.2004	13.8389	13.6989	13.6637
		50	38.4410	24.9597	19.0914	17.3263	16.6995	16.4820	16.4323

Table 10. Nondimensional critical buckling loads of ($0^0/\theta/0^0$) and ($0^0/\theta$) composite beams (MAT I, $E_1/E_2=40$).

Lay-up	BC	*L/h*	Fiber angle (θ)						
			0^0	15^0	30^0	45^0	60^0	75^0	90^0
$0^0/\theta/0^0$	S-S	5	9.2665	9.2022	9.0709	8.9063	8.7542	8.6499	8.6131
		10	19.9125	19.5865	19.3911	19.1853	18.9974	18.8677	18.8217
		50	32.0563	31.1266	30.9641	30.9123	30.8826	30.8653	30.8596
	C-F	5	4.9708	4.8900	4.8413	4.7901	4.7432	4.7109	4.6994
		10	7.0644	6.8878	6.8417	6.8111	6.7856	6.7683	6.7622
		50	8.1715	7.9291	7.8897	7.8801	7.8762	7.8744	7.8739
	C-C	5	12.7118	12.5874	12.3736	12.1114	11.8718	11.7089	11.6517
		10	37.0660	36.8088	36.2838	35.6253	35.0169	34.5997	34.4524
		50	119.0990	115.9313	115.2235	114.8359	114.5322	114.3307	114.2601
$0^0/\theta$	S-S	5	9.2665	6.5269	4.8298	4.2459	4.0242	3.9414	3.9211
		10	19.9125	10.3374	6.5116	5.4620	5.1007	4.9748	4.9455
		50	32.0563	12.7577	7.3361	6.0162	5.5800	5.4319	5.3981
	C-F	5	4.9708	2.5808	1.6246	1.3620	1.2717	1.2405	1.2333
		10	7.0644	3.0334	1.7845	1.4714	1.3672	1.3317	1.3236
		50	8.1715	3.2134	1.8418	1.5094	1.3998	1.3628	1.3543
	C-C	5	12.7118	10.9044	9.6517	9.0600	8.7780	8.6511	8.6154
		10	37.0660	26.1089	19.3221	16.9879	16.1028	15.7733	15.6927
		50	119.0990	49.5841	28.8970	23.7764	22.0782	21.5022	21.3712

Table 11. Nondimensional mid-span displacements of ($0^0/\theta/0^0$) and ($0^0/\theta$) composite beams under a uniformly distributed load (MAT II).

Lay-up	BC	*L/h*	Reference	Fiber angle (θ)						
				0^0	15^0	30^0	45^0	60^0	75^0	90^0
$0^0/\theta/0^0$	S-S	5	Present	1.7930	1.8626	2.0140	2.1762	2.3030	2.3796	2.4049
			Vo et al. [28]	1.7930	1.8626	2.0140	2.1762	2.3030	2.3796	2.4049
		10	Present	0.9222	0.9529	0.9946	1.0370	1.0700	1.0900	1.0965
			Vo et al. [28]	0.9222	0.9529	0.9946	1.0370	1.0700	1.0900	1.0965
		50	Present	0.6370	0.6554	0.6608	0.6634	0.6650	0.6658	0.6661
			Vo et al. [28]	0.6370	0.6554	0.6608	0.6634	0.6650	0.6658	0.6661
	C-F	5	Present	5.2683	5.4840	5.8705	6.2780	6.5930	6.7820	6.8442
			Vo et al. [28]	5.2774	5.4898	5.8804	6.2879	6.6029	6.7919	6.8541
		10	Present	2.9647	3.0636	3.1810	3.2973	3.3871	3.4412	3.4511
			Vo et al. [28]	2.9663	3.0653	3.1828	3.2992	3.3889	3.4428	3.4605
		50	Present	2.1599	2.2225	2.2402	2.2480	2.2529	2.2554	2.2562
			Vo et al. [28]	2.1602	2.2228	2.2405	2.2483	2.2531	2.2557	2.2565
	C-C	5	Present	1.0866	1.1485	1.2616	1.3801	1.4711	1.5253	1.5431
			Vo et al. [28]	1.0998	1.1537	1.2670	1.3856	1.4766	1.5309	1.5487
		10	Present	0.3958	0.4120	0.4459	0.4818	0.5098	0.5266	0.5323
			Vo et al. [28]	0.3968	0.4130	0.4469	0.4828	0.5108	0.5277	0.5332
		50	Present	0.1367	0.1408	0.1431	0.1449	0.1462	0.1470	0.1473
			Vo et al. [28]	0.1367	0.1408	0.1431	0.1449	0.1462	0.1470	0.1472
$0^0/\theta$	S-S	5	Present	1.7930	2.5772	3.6681	4.3236	4.6312	4.7422	4.7645
			Vo et al. [28]	1.7930	2.5763	3.6634	4.3135	4.6135	4.7162	4.7346
		10	Present	0.9222	1.6876	2.7463	3.3492	3.6070	3.6841	3.6942
			Vo et al. [28]	0.9222	1.6861	2.7403	3.3370	3.5871	3.6562	3.6626
		50	Present	0.6370	1.3974	2.4454	3.0309	3.2725	3.3394	3.3446
			Vo et al. [28]	0.6370	1.3966	2.4406	3.0200	3.2540	3.3121	3.3147
	C-F	5	Present	5.2683	7.9931	11.6981	13.8805	14.8708	15.2025	15.2595
			Vo et al. [28]	5.2774	8.0005	11.6830	13.8390	14.8020	15.1080	15.1540
		10	Present	2.9647	5.5734	9.1667	11.2026	12.0630	12.3104	12.3387
			Vo et al. [28]	2.9663	5.5712	9.1499	11.1650	12.0020	12.2260	12.2440
		50	Present	2.1599	4.7445	8.3044	10.2904	11.1059	11.3243	11.3428
			Vo et al. [28]	2.1602	4.7429	8.2916	10.2600	11.0540	11.2500	11.2580
	C-C	5	Present	1.0866	1.3071	1.5673	1.7485	1.8524	1.9023	1.9164
			Vo et al. [28]	1.0998	1.3165	1.5755	1.7547	1.8575	1.9060	1.9193
		10	Present	0.3958	0.5581	0.7797	0.9137	0.9771	1.0003	1.0050
			Vo et al. [28]	0.3968	0.5584	0.7783	0.9107	0.9726	0.9943	0.9983
		50	Present	0.1367	0.2889	0.4987	0.6161	0.6646	0.6778	0.6790
			Vo et al. [28]	0.1367	0.2887	0.4974	0.6137	0.6608	0.6727	0.6733

Table 12. Nondimensional stresses of ($0^0/\theta/0^0$) and ($0^0/\theta$) S-S composite beams under a uniformly distributed load (MAT II).

Lay-up	*L/h*	Reference	Fiber angle (θ)						
			0^0	15^0	30^0	45^0	60^0	75^0	90^0
a. Normal axial stress									
$0^0/\theta/0^0$	5	Present	0.9556	0.9788	1.0062	1.0339	1.0556	1.0688	1.0732
		Vo et al. [28]	0.9498	0.9731	1.0010	1.0280	1.0500	1.0630	1.0670
	10	Present	0.7998	0.8220	0.8325	0.8403	0.8459	0.8493	0.8504
		Vo et al. [28]	0.8002	0.8222	0.8326	0.8403	0.8459	0.8491	0.8502
	50	Present	0.7520	0.7736	0.7785	0.7798	0.7803	0.7805	0.7806
		Vo et al. [28]	0.7523	0.7739	0.7788	0.7801	0.7806	0.7808	0.7809
$0^0/\theta$	5	Present	0.9556	0.5735	0.3736	0.2830	0.2476	0.2386	0.2380
		Vo et al. [28]	0.9498	0.5724	0.3746	0.2852	0.2510	0.2429	0.2428
	10	Present	0.7998	0.5413	0.3655	0.2790	0.2445	0.2354	0.2346
		Vo et al. [28]	0.8002	0.5415	0.3661	0.2802	0.2464	0.2379	0.2375
	50	Present	0.7520	0.5316	0.3631	0.2779	0.2436	0.2344	0.2336
		Vo et al. [28]	0.7523	0.5315	0.3633	0.2785	0.2449	0.2363	0.2358
b. Shear stress									
$0^0/\theta/0^0$	5	Present	0.6668	0.6384	0.5721	0.5010	0.4456	0.4123	0.4013
		Vo et al. [28]	0.6679	0.6395	0.5729	0.5016	0.4462	0.4128	0.4017
	10	Present	0.7078	0.6761	0.6070	0.5330	0.4751	0.4401	0.4286
		Vo et al. [28]	0.7100	0.6783	0.6088	0.5344	0.4762	0.4411	0.4295
	50	Present	0.7439	0.7096	0.6377	0.5609	0.5006	0.4641	0.4521
		Vo et al. [28]	0.7434	0.7090	0.6373	0.5605	0.5003	0.4638	0.4518
$0^0/\theta$	5	Present	0.6668	0.6996	0.7545	0.8155	0.8646	0.8949	0.9052
		Vo et al. [28]	0.6679	0.7050	0.7598	0.8208	0.8703	0.9012	0.9117
	10	Present	0.7078	0.7356	0.7902	0.8532	0.9046	0.9367	0.9476
		Vo et al. [28]	0.7100	0.7394	0.7913	0.8528	0.9039	0.9363	0.9474
	50	Present	0.7439	0.7685	0.8234	0.8884	0.9418	0.9755	0.9869
		Vo et al. [28]	0.7434	0.7443	0.7434	0.7718	0.8085	0.8372	0.8481

Table 13. Fundamental frequencies (Hz) of single-layer C-F composite beam (MAT III).

Lay-up	Theory	Reference	Mode				
			1	2	3	4	5
15^0	HOBT	Present	82.19	512.86	1426.29	-	2767.83
	Quasi-3D	Present	82.22	513.09	1427.12	-	2769.99
		Chen et al. [17]	82.55	515.68	1437.02	-	2797.14
	Experiment	Abarcar and Cunniff [42]	82.50	511.30	1423.40	1526.90*	2783.60
30^0	HOBT	Present	52.63	329.13	918.51	1791.22	-
	Quasi-3D	Present	52.67	329.43	919.48	1793.62	-
		Chen et al. [17]	52.73	330.04	922.45	1803.01	-
	Experiment	Abarcar and Cunniff [42]	52.70	331.80	924.70	1766.90	1827.50*

Note: '-' denotes: the results are not available; '' denotes: the results are the torsional mode*

Table 14. Nondimensional fundamental frequencies of composite beams (MAT IV).

Lay-up	Theory	Reference	BC		
			S-S	C-F	C-C
$45^0/-45^0/45^0/-45^0$	HOBT	Present	0.7961	0.2849	1.7592
		Chandrashekhara and Bangera [36]	0.8278	0.2962	1.9807
	Quasi-3D	Present	0.7962	0.2852	1.7629
		Chen et al. [17]	0.7998	0.2969	1.8446
$30^0/-50^0/50^0/-30^0$	HOBT	Present	0.9726	0.3486	2.1255
	Quasi-3D	Present	0.9728	0.3489	2.1281
		Chen et al. [17]	0.9790	0.3572	2.2640

Table 15. Nondimensional fundamental frequencies, critical buckling loads and mid-span displacements of $(\theta/-\theta)_s$ composite beams (MAT IV).

BC	Theory	Reference	Fiber angle (θ)						
			0^0	15^0	30^0	45^0	60^0	75^0	90^0
a. Fundamental frequency									
S-S	HOBT	Present	2.649	1.579	0.999	0.796	0.731	0.725	0.729
		Aydogdu [20]	2.651	1.896	1.141	0.804	0.736	0.725	0.729
		Nguyen et al. [24]	2.656	2.511	2.103	1.537	1.012	0.761	0.732
	FOBT	Chandrashekhara et al. [6]	2.656	2.511	2.103	1.537	1.012	0.761	0.732
	Quasi-3D	Present	2.650	1.580	0.999	0.796	0.731	0.725	0.730
C-F	HOBT	Present	0.980	0.570	0.358	0.285	0.261	0.259	0.261
		Aydogdu [20]	0.981	0.676	0.414	0.288	0.262	0.258	0.260
		Nguyen et al. [24]	0.983	0.926	0.768	0.555	0.363	0.272	0.262
	FOBT	Chandrashekhara et al. [6]	0.982	0.925	0.768	0.555	0.363	0.272	0.262
	Quasi-3D	Present	0.980	0.571	0.358	0.285	0.262	0.260	0.262
C-C	HOBT	Present	4.897	3.288	2.180	1.759	1.620	1.605	1.615
		Aydogdu [20]	4.973	4.294	2.195	1.929	1.669	1.612	1.619
		Nguyen et al. [24]	4.912	4.717	4.131	3.197	2.202	1.683	1.621
	FOBT	Chandrashekhara et al. [6]	4.849	4.664	4.098	3.184	2.198	1.682	1.620
	Quasi-3D	Present	4.901	3.290	2.183	1.762	1.626	1.614	1.625
		Chen et al. [17]	4.858	3.648	2.345	1.838	1.671	1.616	1.623
b. Critical buckling load									
S-S	HOBT	Present	10.709	3.808	1.522	0.967	0.816	0.802	0.813
	Quasi-3D		10.713	3.809	1.523	0.967	0.816	0.802	0.813
C-F	HOBT	Present	2.973	0.987	0.386	0.244	0.206	0.202	0.205
	Quasi-3D		2.974	0.988	0.387	0.245	0.206	0.203	0.206
	FOBT	Wang et al. [38]	2.971	1.631	0.712	0.298	0.208	0.202	0.205
C-C	HOBT	Present	30.689	13.320	5.747	3.720	3.154	3.096	3.136
	Quasi-3D		30.726	13.336	5.758	3.731	3.168	3.117	3.160
	FOBT	Wang et al. [38]	30.592	19.960	10.008	4.491	3.187	3.098	3.136
c. Mid-span displacement									
S-S	HOBT	Present	1.196	3.371	8.437	13.286	15.745	16.028	15.811
	Quasi-3D		1.195	3.369	8.432	13.278	15.733	16.014	15.796
C-F	HOBT		3.987	11.387	28.611	45.097	53.452	54.413	53.675
	Quasi-3D		3.983	11.378	28.570	44.967	53.170	54.010	53.208
C-C	HOBT		0.355	0.795	1.815	2.791	3.289	3.350	3.308
	Quasi-3D		0.355	0.794	1.812	2.782	3.272	3.322	3.276